J|A|C|S
ARTICLES
Published on Web 08/19/2006

Femtosecond Time- and Wavelength-Resolved Fluorescence and Absorption Spectroscopic Study of the Excited States of Adenosine and an Adenine Oligomer

Wai-Ming Kwok,* Chensheng Ma, and David Lee Phillips*

Contribution from the Department of Chemistry, The University of Hong Kong, Pokfulam Road, Hong Kong S. A. R., P. R. China

Received March 31, 2006; E-mail: kwokwm@hkucc.hku.hk; phillips@hkucc.hku.hk

Abstract: By employing broadband femtosecond Kerr-gated time-resolved fluorescence (KTRF) and transient absorption (TA) techniques, we report the first (to our knowledge) femtosecond combined time- and wavelength-resolved study on an ultraviolet-excited nucleoside and a single-stranded oligonucleotide (namely adenosine (Ado) and single-stranded adenine oligomer $(dA)_{20}$) in aqueous solution. With the advantages of the ultrafast time resolution, the broad spectral and temporal probe window, and a high sensitivity, our KTRF and TA results enable the real time monitoring and spectral characterization of the excited-state relaxation processes of the Ado nucleoside and $(dA)_{20}$ oligonucleotide investigated. The temporal evolution of the 267 nm excited Ado KTRF spectra indicates there are two emitting components with lifetimes of ~0.13 ps and ~0.45 ps associated with the L_a and L_b $\pi\pi^*$ excited states, respectively. These Ado results reveal no obvious evidence for the involvement of the $n\pi^*$ state along the irradiative internal conversion pathway. A distinct mechanism involving only the two $\pi\pi^*$ states has been proposed for the ultrafast Ado deactivation dynamics in aqueous solution. The time dependence of the 267 nm excited $(dA)_{20}$ KTRF and TA spectra reveals temporal evolution from an ultrafast "A-like" state (with a ~0.39 ps decay time) to a relatively long-lived E_1 "excimer" (~4.3 ps decay time) and an E_2 "excimer-like" (~182 ps decay time) state. The "A-like" state has a spectral character closely resembling the excited state of Ado. Comparison of the spectral evolution between the results for Ado and $(dA)_{20}$ provides unequivocal evidence for the local excitation character of the initially photoexcited $(dA)_{20}$. The rapid transformation of the locally excited $(dA)_{20}$ component into the delocalized E_1 "excimer" state which then further evolves into the E_2 "excimer-like" state indicates that base stacking has a high ability to modify the excited-state deactivation pathway. This modification appears to occur by suppressing the internal conversion pathway of an individually excited base component where the stacking interaction mediates efficient interbase energy transfer and promotes formation of the collective excited states. This feature of the local excitation that is subsequently followed by rapid energy delocalization into nearby bases may occur in many base multimer systems. Our results provide an important new contribution to better understanding DNA photophysics.

Introduction

Since solar ultraviolet (UV) irradiation of DNA can produce DNA excited states that may undergo photochemical events leading to base damage and genetic modification,[1] there have been extensive studies for more than four decades aiming to understand the photophysics and photochemistry of UV-excited DNA.[1−4] It is now well established that, as the building blocks of DNA, the nucleic acid bases are remarkably photostable due to their ultrashort excited-state lifetimes (<1 ps) brought about by an ultrafast irradiative internal conversion (IC) pathway of the singlet excited states.[5−12] However, the dynamics and outcome of UV-excited DNA and base multimers have been found to be quite complicated and sensitive to many factors such as base sequences, base modifications, base pairing, and base stacking, etc.[4,13−20] A recent femtosecond excited-state absorption (fs-ESA) study by Kohler and co-workers on adenine

(1) Cadet, J.; Vigny, P. In *The Photochemistry of Nucleic Acid in Bioorganic Photochemistry*; Morrison, H., Ed.; John Wiley & Sons: New York, 1990; pp 1−272.
(2) Nikogosyan, D. N. *Int. J. Radiat. Biol.* **1990**, *57*, 233−299
(3) Burrows, C. J.; Muller, J. G. *Chem. Rev.* **1998**, *98*, 1109−1152
(4) Crespo-Hernández, C. E.; Cohen, B.; Hare, P. M.; Kohler, B. *Chem. Rev.* **2004**, *104*, 1977−2019.
(5) (a) Pecout, J.-M. L.; Peon, J.; Kohler, B. *J. Am. Chem. Soc.* **2000**, *122*, 9348−9349. (b) Pecout, J.-M. L.; Peon, J.; Kohler, B. *J. Am. Chem. Soc.* **2001**, *123*, 10370−10378. (c) Cohen, B.; Hare, P. M.; Kohler, B. *J. Am. Chem. Soc.* **2003**, *125*, 13594−13601.
(6) Kuimova, M. K.; Dyer, J.; George, M. W.; Grill, A. C.; Kelly, J. M.; Matousek, P.; Parker, A. W.; Sum, X. Z.; Towrie, M.; Whelan, A. M. *Chem. Commun.* **2005**, 1182−1184.
(7) Peon, J.; Zewail, A. H. *Chem. Phys. Lett.* **2001**, *348*, 255−262.
(8) Onidas, D.; Markovitsi, D.; Marguet, S.; Sharonov, A.; Gustavsson, T. *J. Phys. Chem. B* **2002**, *106*, 11367−11374.
(9) Pancur, T.; Schwalb, N. K.; Renth, F.; Friedrich, T. *Chem. Phys.* **2005**, *313*, 199−212.
(10) Ullrich, S.; Schultz, T.; Zgierski, A. Z.; Stolow, A. *J. Am. Chem. Soc.* **2004**, *126*, 2262−2263.
(11) Kang, H.; Lee, K. T.; Jung, B.; Ko, Y. J.; Kim, S. K. *J. Am. Chem. Soc.* **2002**, *124*, 12958−12959.
(12) Perun, S.; Sobolewski, A. L.; Domcke, W. *J. Am. Chem. Soc.* **2005**, *127*, 6257−6265.
(13) (a) Crespo-Hernández, C. E.; Cohen, B.; Kohler, B. *Nature* **2005**, 436, 1141−1144. (b) Crespo-Hernández, C. E.; Kohler, B. *J. Phys. Chem. B* **2004**, *108*, 11182−11188.

 10.1021/ja0622002 CCC: $33.50

and adenine-thymine oligonucleotides reported a high yield of a long-lived (with ~126 ps lifetime) "excimer" state. From comparison of the "excimer" dynamics observed for the single-stranded and corresponding double-stranded oligomers, they concluded that the base stacking is predominant in controlling the excited-state dynamics for these systems.[13a] Since the relatively long "excimer" lifetime may increase its propensity toward photochemical reaction, there has been some expectation that there is a direct link of this state to some of the important photolesions observed in living cells.[13,21−23] The "excimer" state was suggested to be formed as a result of interbase π stacking coupling with excitation delocalized among the interacting bases.[4,20] The "excimer" state has a characteristic red-shifted fluorescence (λ_{max} at ~380−400 nm) relative to the monomer fluorescence (λ_{max} at ~310 nm) and was first discovered in low-temperature emission experiments by Eisinger and co-workers in 1966[20a] and has been observed later in diverse di-, oligo-, and polynucleotides.[13,15,19,22,24] These results are consistent with the importance of base stacking in mediating the delocalization of the energy after photoexcitation and influencing the excited-state deactivation pathway. However, there is no clear picture to describe the direct dynamics relating the stacking interaction to the excitation relaxation of UV-excited base multimers. One fundamental and unresolved question concerns the origination of the long-lived "excimer" state: it is unclear whether this state originates from a statically delocalized excited exciton state or is formed dynamically after local excitation of the component base unit. The latter description is favored by many studies as indicated obviously by the use of the "excimer" term.[13,15,20] But the former description has been suggested by steady-state fluorescence polarization and excitation measurements on natural base constituted multimers[14a,19,25,26] and 2-aminopurine (2AP) incorporated oligonucleotides[27] and is also supported by several recent theoretical calculations.[28] To address and clarify this issue, it would be important to acquire direct spectral and dynamical information for the excited states of both the nucleobase constituents and the corresponding base multimers. While recent ultrafast time-resolved studies[4−11,13−16] have contributed greatly to the description of the dynamics of the excited states, there has been very little combined time- and wavelength-dependent spectral evidence available (particularly on the femtosecond time scale) in the literature for the excited states of a single base and its related base mulitmer.[15,24] The lack of this important data is due to many experimental difficulties associated with the intrinsic properties of these systems including the extremely low room-temperature fluorescence quantum yield (~10^{-5}−10^{-4}),[1,2,4,8,13b,29] broad spectral coverage,[15,19,20,22,24] substantial overlap of the monomer and "excimer" fluorescence,[20,22] and remarkable differences in the lifetimes between the excited monomer and "excimer" state.[4,5−11,13,14,15] To help fill in this gap, we have utilized our recently developed broadband Kerr-gated time-resolved fluorescence (fs-KTRF) and transient absorption (fs-TA) techniques[30] to perform the first combined femtosecond time-resolved and wavelength-resolved fluorescence and transient absorption spectroscopic study on the adenine monomer adenosine (Ado) and oligonucleotide $(dA)_{20}$ consisting of 20 consecutive 2′-deoxyadenosine (dA) residues. The excited-state temporal evolution of the two systems has been monitored and compared within a broad spectral and temporal probe window.

Adenine is the most extensively studied DNA base.[4−12,31−34] The gas-phase deactivation pathway of UV-excited adenine has been well characterized[10,11,31] and attributed to conical intersections due to crossing of the $\pi\pi^*$ and $n\pi^*$ excited states to the ground-state potential surface.[12,32−34] Although the gas-phase studies show that the very short excited-state lifetime is an intrinsic property of the DNA bases,[10,11] there have been several experimental investigations[5b,8,9] which found that the adenine deactivation dynamics in aqueous solution are shorter and do not exhibit the pronounced excitation wavelength dependence that is observed in the adenine gas-phase experiment.[11] This indicates the importance of solvent effects on influencing the excited-state relaxation process. Since the solvent can modify and even reorder the $\pi\pi^*$ and $n\pi^*$ energy levels,[30a,35,36] it has remained an open question about the precise mechanism and identity of the particular excited state(s) responsible for the solution phase adenine ultrafast deactivation. The adenine-constituted oligo- and polynucleotides are among the best-stacked base multimers[37,38] and exhibit a high propensity for generating the "excimer" state after UV excitaiton.[13,15,22] At room temperature in neutral aqueous solution conditions used here for our KTRF and TA measurements, $(dA)_{20}$, like the homopolymer poly(2′-deoxyadenylic acid) (poly(dA)),[38] is mostly in the single-stranded form with ~80% of the adenine

(14) (a) Markovitsi, D.; Onidas, D.; Gustavsson, T.; Talbot, F.; Lazzarotto, E. *J. Am. Chem. Soc.* **2005**, *127*, 17130−17131. (b) Markovitsi, D.; Sharonov, A.; Onidas, D.; Gustavsson, T. *ChemPhysChem* **2003**, *3*, 303−305.
(15) Plessow, R.; Brockhinke, A.; Eimer, W.; Kohse-Höinghaus, K. J. *Phys. Chem. B* **2000**, *104*, 3695−3704.
(16) Fiebig, T.; Wan, C.; Zewail, A. H. *ChemPhysChem* **2002**, *3*, 781−788.
(17) Xu, D.; Nordlund, T. M. *Biophys. J.* **2000**, *78*, 1042−1058.
(18) Huang, C.; Georghiou, S. *Photochem. Photobiol.* **1992**, *56*, 95−99.
(19) (a) Ballini, J.-P.; Daniels, M.; Vigny, P. *Biophys. Chem.* **1991**, *39*, 253−265. (b) Ballini, J.-P.; Vigny, P.; Daniels, M. *Biophys. Chem.* **1983**, *18*, 61−65.
(20) (a) Eisinger, J.; Guéron, M.; Shulman, R. G.; Yamane, T. *Proc. Natl. Acad. Sci. U.S.A.* **1966**, *55*, 1015−1020. (b) Guéron, M.; Eisinger, J.; Shulman, R. G. *Proc. Natl. Acad. Sci. U.S.A.* **1966**, *56*, 814−818. (c) Eisinger, J.; Shulman, R. G. *Science* **1968**, *161*, 1311−1319.
(21) Lamola, A. A.; Eisinger, J. *Proc. Natl. Acad. Sci. U.S.A.* **1968**, *59*, 46−51.
(22) Vigny, P.; Ballini, J. P. In *Excited State in Organic Chemistry and Biochemistry*; Pullman, B., Goldblum, N., Eds.; D. Reidel: Dordrecht, The Netherlands, 1977.
(23) Pechenaya, V. I.; Danilov, V. I.; Slyusarchuk, O. N.; Alderfer, J. L. *Photochem. Photobiol.* **1995**, *61*, 435−441.
(24) Kobayashi, S.; Yamashita, M.; Sato, T.; Muramatsu, S. *IEEE J. Quantum Electron.* **1984**, *QE-20*, 1383−1385.
(25) Wllson, R. W.; Callis, P. R. *J. Phys. Chem.* **1976**, *80*, 2280−2288.
(26) Kononov, A. I.; Bukina, M. N. *J. Biomol. Struct. Dyn.* **2002**, *20*, 465−471.
(27) Rist, M.; Wagenknecht, H.-A.; Fiebig, T. *ChemPhysChem.* **2002**, *8*, 704−707.
(28) (a) Emanuele, E.; Markovitsi, D.; Millié, P.; Zakrzewska, K. *ChemPhysChem.* **2005**, *6*, 1387−1392. (b) Emanuele, E.; Zakrzewska, K.; Markovitsi, D.; Lavery, R.; Millié, P. *J. Phys. Chem.* **2005**, *109*, 16109−16118. (c) Bouvier, B.; Dognon, J.-P.; Lavery, R.; Markovitsi, D.; Millié, P.; Onidas, D.; Zakrzewska, K. *J. Phys. Chem.* **2003**, *107*, 13512−13522. (d) Bouvier, B.; Gustavsson, T.; Markovitsi, D.; Millié, P. *Chem. Phys.* **2002**, *275*, 75−92.
(29) Daniels, M.; Hauswirth, W. *Science* **1971**, *171*, 675−677.
(30) (a) Ma, C.; Kwok, W. M.; Chan, W. S.; Zuo, P.; Kan J. T. W.; Toy, P. H.; Phillips, D. L. *J. Am. Chem. Soc.* **2005**, *127*, 1463−1427. (b) Ma, C.; Kwok, W. M.; Chan, W. S.; Du, Y.; Kan J. T. W.; Toy, P. H.; Phillips, D. L. *J. Am. Chem. Soc.* **2006**, *128*, 2558−2570. (c) Zuo, P.; Ma, C.; Kwok, W. M.; Chan, W. S.; Phillips, D. L. *J. Org. Chem.* **2005**, *70*, 8661−8675.
(31) Canuel, C.; Mons, M.; Piuzzi, F.; Iardivel, B.; Dimicoli, I, Elhanine, M. *J. Chem. Phys.* **2005**, *122*, No. 074316.
(32) Blancafort, L. *J. Am. Chem. Soc.* **2006**, *128*, 210−219.
(33) Chen H.; Li, S. *J. Phys. Chem. A* **2005**, *109*, 8443−8446.
(34) Marian, C. M. *J. Chem. Phys.* **2005**, *122*, No. 104314.
(35) (a) Holmén, A.; Broo, A.; Albinsson, B.; Nordén, B. *J. Am. Chem. Soc.* **1997**, *119*, 12240−12250. (b) Holmén, A.; Nordén, B.; Albinsson, B. *J. Am. Chem. Soc.* **1997**, *119*, 3114−3121. (c) Albinsson, B.; Nordén, B. *J. Am. Chem. Soc.* **1993**, *115*, 223−231.
(36) Mennucci, B.; Toniolo, A.; Tomasi, J. *J. Phys. Chem.* **2001**, *105*, 4749−4757.
(37) Powell, J. T.; Richards, E. G.; Gratzer, W. B. *Biopolymers* **1972**, *11*, 235−250.
(38) Dewey, T. G.; Turner, D. H. *Biochemistry* **1979**, *18*, 5757−5762.

bases stacked. In this sense, adenine and $(dA)_{20}$ are archetypal systems for making a comparative study to explore the relationship between the excited states of base constituents and their interaction with nearby bases in the stacked DNA. Ado was chosen in the present study to avoid the spectral complexity associated with the existence of the 9H and 7H tautomers in adenine: by attaching a ribose moiety at the 9 position, the tautomer 7H configuration is ruled out in Ado.[4,5,9] We note that previous time-resolved studies on adenine oligo- and polynucleotides report generally multiexponential excited-state decay dynamics but with correlating time constants and spectral components varying strongly due to differences in experimental methods, time resolution, and width of the spectral and time detection windows.[13,14b,15,24,39] Employing the combined advantages of femtosecond time resolution, a broad detection window, and a high sensitivity, our KTRF and TA spectroscopic study enables a significantly improved characterization of the spectral band shapes and their dynamics for UV-excited Ado and $(dA)_{20}$.

Our results for the excited-state dynamics allow a straightforward comparison with previous relevant investigations, and more importantly, the novel information on the temporal evolution of the spectral profile provides crucial evidence for deciphering the evolution of the excited states through different electronic configurations for Ado and $(dA)_{20}$. Based on our new time-resolved spectroscopy results and steady-state absorption and fluorescence measurements, we propose an alternative mechanism to account for the aqueous solution Ado ultrafast deactivation. From comparison of the results obtained for Ado and $(dA)_{20}$, our data enable an explicit assessment of the origin of the long-lived oligomer excited state and provides the first evidence-based description of the excitation relaxation pathway for adenine nucleotides.

Experimental Method

Both the fs-KTRF and fs-TA measurement were performed based on a commercial Ti:Sapphire regenerative amplifier laser system.[30,40] The samples (aqueous solution of ~2 mM concentration) were excited by a femtosecond pump laser pulse in the UV at 267 nm (the third harmonic of the 800 nm regenerative amplifier fundamental). The subsequent relaxation of the induced excited states was followed by a second femtosecond probe pulse that monitors the temporal evolution of the transient fluorescence and absorption spectrum by the KTRF[30a] and TA[30b,c] spectroscopy, respectively. In the fs-KTRF measurements, a Kerr-gate technique[41] was employed. The Kerr medium (a 1 mm thick fused silica plate) equipped with a crossed polarizer pair is driven by a 800 nm gating pulse (as a probe) to act as an ultrafast shutter to sample the excited-state fluorescence spectra at various pump/probe delay times. In our fs-TA experiments, the sample was probed by a white light continuum pulse created from a rotating CaF_2 plate pumped by the 800 nm fundamental laser pulse. The time window for both the KTRF and TA measurements extends from fs to ~2 ns. The spectral window of our KTRF and TA measurements covers the ~270−700 nm and the 300−700 nm regions, respectively. The instrument response function (IRF) of our ultrafast system is wavelength-dependent and varies from ~250 fs to ~350 fs for KTRF and ~150 fs to ~250 fs for TA as the wavelength varies from 600 to 280 nm. To avoid introducing unwanted multiphoton or saturation effects, the power of the pump laser pulse is kept as low as possible and a typical laser pulse peak power used for the KTRF and TA experiments is ~2 GW/cm^2. For details of the KTRF and TA experimental setups and the related spectral calibrations, the reader is referred to refs 30 and 41. In the TA measurements, the raw data of the measured TA spectra contain an overlapping contribution from the sample (Ado or $(dA)_{20}$) and the solvated electron[5,13] in the aqueous solution. The sample spectra shown in Figures 5 and 6 were acquired by subtracting the TA spectra of the solvated electron (obtained in blank water solvent under the same pump/probe conditions) from the raw spectra obtained in the sample solution (see Figure 1S in the Supporting Information for details of the spectral subtraction).

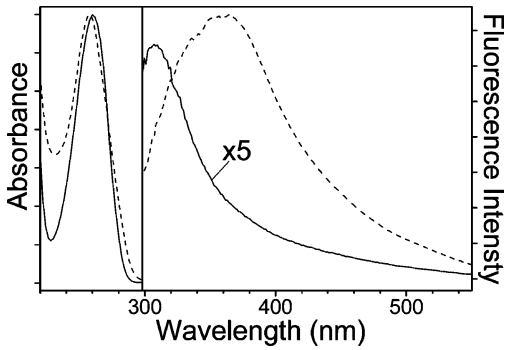

Figure 1. Normalized steady-state UV absorption spectra and 267 nm excited fluorescence spectra of Ado (solid line) and $(dA)_{20}$ (dotted line) in an aqueous solution. The weak Ado fluorescence spectrum was enlarged by 5 times for clear comparison.

The steady-state UV absorption spectra were measured by using a Perkin-Elmer Lambda 19 UV/vis spectrometer. The steady-state fluorescence spectra were recorded utilizing our KTRF setup but operated in a steady-state mode by removal of the pair of crossed polarized and the Kerr medium. The spectra were calibrated with reference to a known standard sample.

The Ado sample was purchased from Fluka (with >99% purity), and the $(dA)_{20}$ was purchased from Sigma Proligo with RPC purification (~90% purity). The compounds were used without further purification. Solutions of tridistillated water were used for the experiments. The UV-melting curve measured for $(dA)_{20}$ in aqueous solution (displayed in Figure 2S in the Supporting Information) suggests that ~80% of the adenine bases are stacked at room temperature (23 °C). This is very close to the stacking percentage (~79%) reported in a previous temperature-jump study for poly(dA).[38] On the other hand, the UV-absorption measurement for Ado in water reveals an unchanged extinction coefficient for the absorption spectrum upon variation of the Ado concentration (0.04−15 mM). This implies that the individual Ado molecules do not stack with each other appreciably even at a nearly saturated concentration (~15 mM). UV absorption spectra obtained before and after the experiments reveal no degradation of the sample during all of the steady-state and time-resolved measurements.

Results

A. Steady-State Absorption and Fluorescence Spectroscopy. The steady-state absorption and fluorescence spectra of Ado and $(dA)_{20}$ are displayed in Figure 1. The absorption spectra of both compounds have been normalized to the intensity maximum of the long wavelength absorption band. The $(dA)_{20}$ absorption spectrum appears similar to the Ado spectrum but with the $(dA)_{20}$ absorption maximum slightly blue-shifted and the low energy edge slightly red-shifted compared to the Ado absorption spectrum. These differences in the absorption spectra of the base monomers to their related stacked base multimers

(39) (a) Ballini, J.-P.; Daniels, M.; Vigny, P. *J. Lumin.* **1982**, *27*, 389−400. (b) Morgan, J. P.; Daniels, M. *Photochem. Photobiol.* **1980**, *31*, 101−113.
(40) (a) Ma, C.; Chan, W. S.; Kwok, W. M.; Zuo, P.; Phillips, D. L. *J. Phys. Chem. B* **2004** *108*, 9264−9276. (b) Kwok, W. M.; Zhao, C.; Li, Y.-L.; Guan, X.; Wang, D.; Phillips, D. L. *J. Am. Chem. Soc.* **2004**, *126*, 3119−3131. (c) Kwok, W. M.; Chan, P. Y.; Phillips, D. L. *J. Phys. Chem. B* **2004**, *108*, 19068−19075.
(41) (a) Matousek, P.; Towrie, M.; Parker, A. W. *Appl. Spectrosc.* **1999**, *53*, 1485−1489. (b) Matousek, P.; Towrie, M.; Ma, C.; Kwok, W. M.; Phillips, D.; Toner, W. T.; Parker, A. W. *J. Raman Spectrosc.* **2001**, *32*, 983−988.

have been observed generally in relevant systems and have been associated with the exciton interaction induced by the close proximity of the stacking bases.[1,4,42,43] It is important to mention that, besides the subtle changes in the spectral profile, the stacking coupling also causes hypochromism of the long wavelength absorption band of the stacked base multimer relative to the base monomer.[43−45] For adenine oligo- and polynucleotides, the loss of the oscillator strength due to the hypochromic effect is around ∼15−30%.[37,38,39b] The fluorescence spectra shown in Figure 1 for Ado and $(dA)_{20}$ were recorded from solutions with an identical absorption at the 267 nm excitation wavelength. The absolute room-temperature fluorescence quantum yield (ϕ_f) of Ado was determined previously to be 6×10^{-5}.[8,42] From the ratio of the area covered by the fluorescence spectra, the ϕ_f of $(dA)_{20}$ can be estimated to be $\sim 6 \times 10^{-4}$, and this value is close to the 7.3×10^{-4} ϕ_f reported for poly(dA).[13b] Comparison of the Ado and $(dA)_{20}$ fluorescence spectra indicates clearly that the ∼10 times larger ϕ_f for $(dA)_{20}$ relative to that for Ado is mainly due to the large extra contribution of the red-shifted fluorescence (λ_{max} at ∼390 nm) exhibited by $(dA)_{20}$ but not by Ado. The red-shifted fluorescence has been ascribed to an "excimer" state by some studies[15,20] but associated alternatively to excitation of stacked complexes with different stacking conformations by other investigations.[26,39]

B. Femtosecond Broadband Kerr-Gated Time-Resolved Fluorescence (fs-KTRF) Spectroscopy. Figure 2a displays the 3D contour of the KTRF spectra for Ado obtained after 267 nm excitation in an aqueous solution with a time delay up to ∼2 ps. The transient fluorescence spectra recorded at time delays of 0.05, 0.4, 1, and 2 ps are displayed in Figure 2c−f. The short lifetime of the excited state(s) is shown clearly by the observation that no fluorescence signal can be detected at a time delay of ∼3 ps and beyond. Although the overall fluorescence profiles appear to be one broad band with a λ_{max} around 310 nm and a long tail extending to ∼550 nm and beyond, the temporal evolution of the spectrum reveals changes in spectral profile on going from early to later time delays. This can be seen clearly by comparison of the spectra at 0.05 ps (Figure 1c) and 2 ps (Figure 1f) delay times. Consistent with this, kinetic analysis found that the dynamic features of the fluorescence decay vary significantly with a change in the fluorescence wavelength. For instance, the temporal decay of the fluorescence slows down gradually on going from the blue to red side of the spectra. A typical example of this is displayed in Figure 2b that shows a comparison of the time profile of the fluorescence decay at the 310 and 420 nm wavelengths. Appropriate simulations of the decay curves require a sum of two exponential functions convoluted with the IRF of our KTRF system. Global analysis of the spectra indicates that the decay dynamics at all fluorescence wavelengths can be simulated satisfactorily by two exponentials with a time constant of 0.13 ps (τ_1) and 0.45 ps (τ_2), respectively, weighted by different proportionality factors. These results are consistent with and in good agreement with similar results reported recently in a single wavelength fluorescence up-conversion study that found a biexponential decay

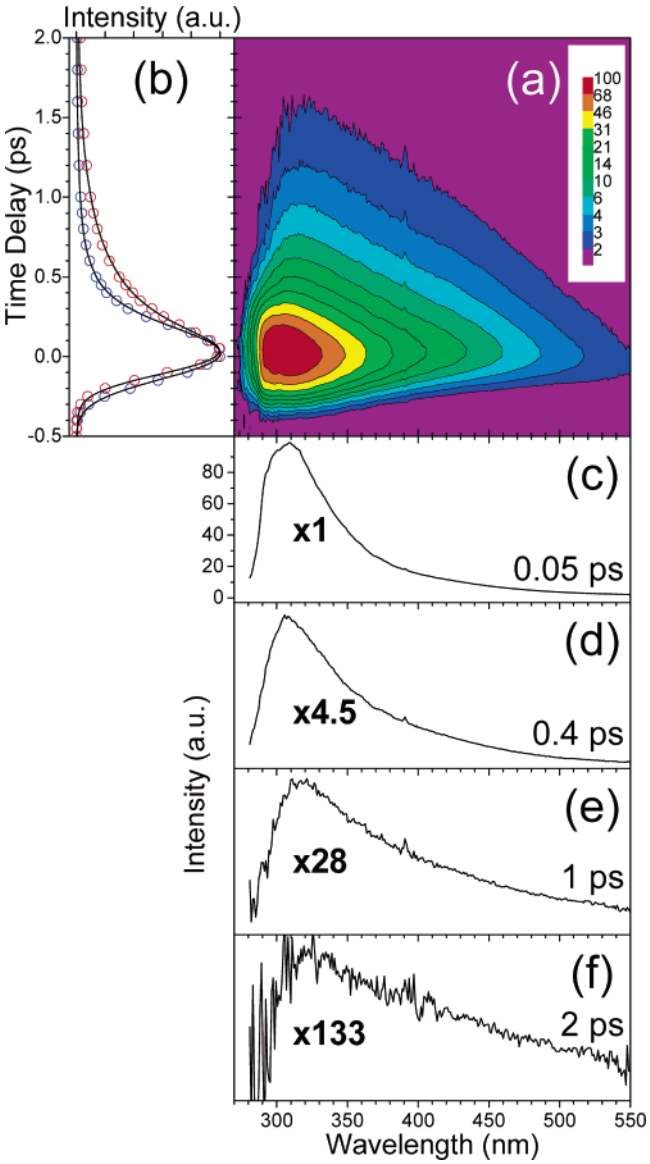

Figure 2. (a) Kerr-gated time-resolved fluorescence contour of Ado obtained with 267 nm excitation in an aqueous solution. (b) Normalized fluorescence decay at 310 nm (circles in blue) and 420 nm (circles in red). The solid lines show the IRF convoluted with a two-exponential function fitting to the experimental data (see text for details). (c−f) Transient fluorescence profiles recorded at typical pump−probe time delays. The spectra in (d−f) have been enlarged differently to display the time-dependent changes in the corresponding spectral profiles.

of 2′-deoxyadenosine at ∼330 nm with time constants of ∼0.10 ps and ∼0.42 ps, respectively.[8] Since the ribose group does not absorb at wavelengths greater than 200 nm,[1,4,8,42] it is straightforward to assign the adenine moiety of Ado as the chromophore responsible for the 267 nm excitation and the observed fluorescence spectra.

The corresponding 3D contour for the KTRF spectra of $(dA)_{20}$ is displayed in Figure 3a with time delays up to 20 ps. Representative transient fluorescence spectra recorded at several typical time delays are displayed in Figure 3c−g. Obviously, in contrast to the ultrafast deactivation dynamics observed for Ado (see Figure 2), the $(dA)_{20}$ fluorescence persists up to hundreds of picoseconds and this indicates the existence of long-lived emitting state(s) formed exclusively after the 267 nm photoexcitation of the multimer. The $(dA)_{20}$ KTRF spectral

(42) Callis, P. R. *Annu. Rev. Phys. Chem.* **1983**, *34*, 329−357.
(43) Kononov, A. I.; Bakulev, V. M.; Rapoport, V. L. *J. Photochem. Photobiol., B* **1993**, *19*, 139−144.
(44) Tinoco, I. *J. Am. Chem. Soc.* **1960**, *82*, 4785−4789.
(45) Rhodes, W. *J. Am. Chem. Soc.* **1961**, *83*, 3609−3617.

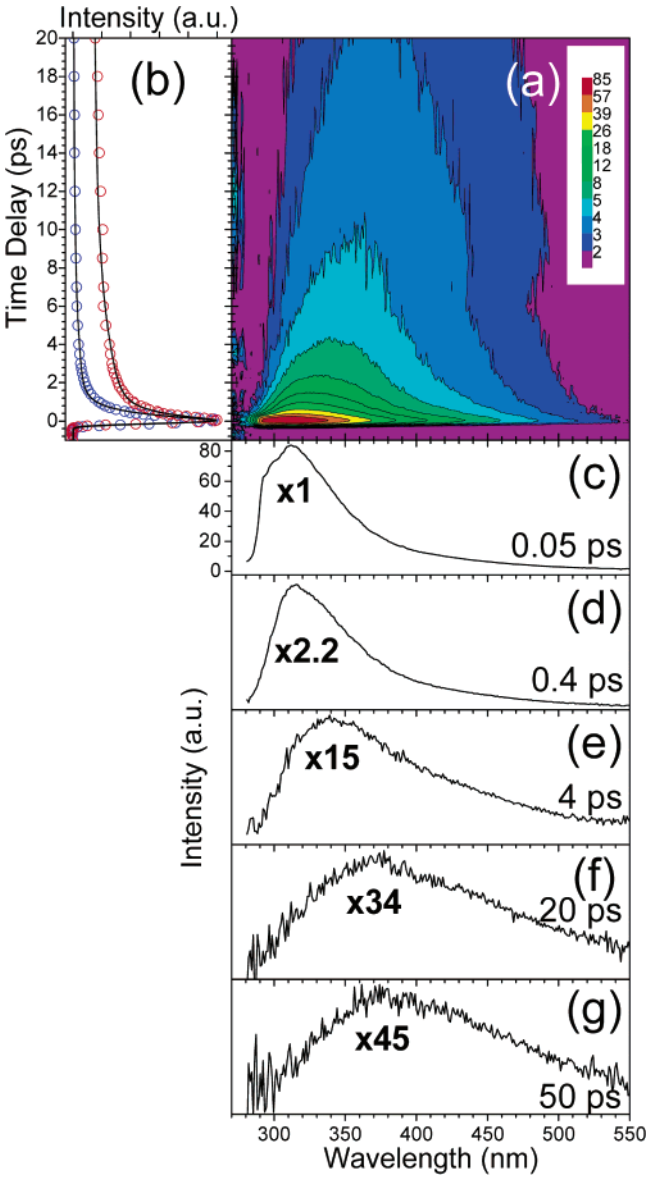

Figure 3. (a) Kerr-gated time-resolved fluorescence 3D-contour of $(dA)_{20}$ obtained with 267 nm excitation in aqueous solution. (b) Normalized fluorescence decay at 310 nm (circles in blue) and 420 nm (circles in red). The solid lines show the IRF convoluted with a three-exponential function fitting to the experimental data (see text for details). (c−g) Transient fluorescence profiles recorded at typical pump−probe time delays. The spectra in (d−g) have been enlarged differently to better display the time-dependent changes in the corresponding spectral profiles.

evolution is characterized by an apparent spectral red shift accompanied by a substantial decrease in spectral intensity. The temporal evolution of the transient fluorescence profile combined with the wavelength-dependence of the intensity decay dynamics indicates there is a three-stage relaxation process associated with three fluorescing components featured by distinct spectral profiles and decay time constants. The fluorescence decay profiles differ remarkably at each wavelength and display much longer decay times as the spectral wavelength is increased. Global analysis of the fluorescence intensity decay at various wavelengths indicates a satisfactory fitting requires three exponential functions with time constants of ~0.39 (τ_1), 4.3 (τ_2), and 182 ps (τ_3). Typical experimental and fitting results of the decay data at wavelengths of 310 and 420 nm within the 20 ps time regime are shown in Figure 3b. The corresponding

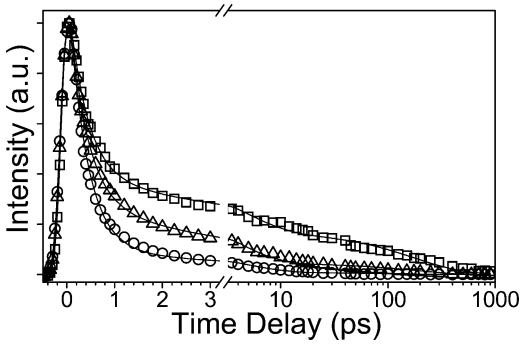

Figure 4. Normalized time-dependence of the fluorescence decay dynamics of 267 nm photoexcited $(dA)_{20}$ at 310 nm (circles), 350 nm (triangles), and 420 nm (squares) resulting from the KTRF spectra displayed in Figure 3a. The solid lines represent the IRF convoluted three-exponential function fitting to the experimental data. The data with time delays before and after 3 ps are displayed, respectively, on a linear and logarithmic time axis.

Table 1. Spectral Parameters of the Excited State Lifetime (τ), the Fluorescence Peak Position (λ_1^{fluo}), the Radiative Rate (k), and the Fluorescence Quantum Yield (ϕ) Obtained from the Steady-State, KTRF, and TA Spectral Analysis of Ado and $(dA)_{20}$ in an Aqueous Solution

	Ado[a]	$(dA)_{20}$[b]
τ_1 (ps)	0.13	0.39
τ_2 (ps)	0.45	4.3
τ_3 (ps)		182
λ_1^{fluo} (nm)	307	310
λ_2^{fluo} (nm)	344	348
λ_3^{fluo} (nm)		390
k_1 ($\times 10^8$ s^{-1})	2.32	0.7
k_2 ($\times 10^8$ s^{-1})	0.57	0.14
k_3 ($\times 10^8$ s^{-1})		0.04
ϕ_{cal} ($\times 10^{-4}$)	0.56	
ϕ_{exp} ($\times 10^{-4}$)	0.6[c]	6

[a] For Ado, values corresponding to τ_1, λ_1^{fluo}, and k_1 are for the L_a state, while those corresponding to τ_2, λ_2^{fluo}, and k_2 are for the L_b state. [b] For $(dA)_{20}$, values corresponding to τ_1, λ_1^{fluo}, and k_1 refer to the "A-like" state, while those corresponding to τ_2, λ_2^{fluo}, and k_2 are for the E_1 state and those corresponding to the τ_3, λ_3^{fluo}, and k_3 are for the E_2 state. [c] From ref 42.

time-dependent results for fluorescence decay at 310, 350, and 420 nm over a time scale up to 1000 ps are displayed in Figure 4. The spectra shown in Figure 3c, e, and f/g at time delays of 0.05 ps, 4 ps, and 20/50 ps can be considered approximately as representative spectra for the three fluorescent components with lifetimes correlating to the time constants determined by the dynamics fitting analysis. It can be seen that the spectrum of the first ultrafast component (see Figure 3c) is strong with a λ_{max} at ~310 nm. In contrast, the spectra of the two later components (the ~4 and 20 ps spectra) are both much weaker and red-shifted compared to the spectrum of the first component (the early 0.05 ps spectrum). The ~4 and 20 ps spectra have maximum intensities of only ~7% and ~3% of that of the early 0.05 ps spectrum, respectively. The ~4 and 20 ps spectra have λ_{max} at ~350 nm and ~390 nm, respectively. Detailed spectral parameters for the three components obtained by simulating the spectra using log-normal functions[46] are presented in Figure 3S and Table 1S in the Supporting Information.

We note that the reconstructed overall fluorescence spectra of Ado and $(dA)_{20}$ obtained based on the recorded corresponding KTRF spectra reproduces quite well the steady-state fluorescence spectra displayed in Figure 1. This indicates that the

(46) Horng, M. L.; Gardecki, J. A.; Papazyan, A.; Maroncelli, M. *J. Phys. Chem.* **1995**, *99*, 17311−17337

transient fluorescence components and the correlated excited states revealed by the KTRF results are the predominant contributors to the steady-state fluorescence. This implies that the two red-shifted and long-lived $(dA)_{20}$ components, especially the one with a λ_{max} at ~390 nm and ~182 ps lifetime, are the major sources of the additional $(dA)_{20}$ red fluorescence observed in the steady-state spectrum and account for the much larger ϕ_f in $(dA)_{20}$ compared to Ado.

When making comparisons between the KTRF results for Ado (Figure 2) and those for $(dA)_{20}$ (Figure 3), it is remarkable that the initial spectra of $(dA)_{20}$ (Figure 3c) and Ado (Figure 2c) exhibit very similar spectral profiles and comparable intensities. This suggests strongly that the early $(dA)_{20}$ fluorescence component originates from an adenine-like (denoted as "A-like" hereafter) excited state with an intrinsic electronic nature close to that of the Ado excited state. In addition, since the KTRF spectra displayed for the two compounds were recorded from solutions with a nearly identical absorbance at the 267 nm excitation wavelength, the analogous intensity exhibited by the Ado and $(dA)_{20}$ early-time spectra indicates that the adenine constituent of $(dA)_{20}$, in both the stacked and unstacked regions, is the predominant chromophore accounting for the overall excitation absorption and the initial fluorescence transitions. As most adenines in $(dA)_{20}$ are in the stacked form,[37,38] it is reasonable that the main part of the excitation and the initial $(dA)_{20}$ fluorescence may be from the stacked adenines. The probability that only the unstacked adenines are responsible for the $(dA)_{20}$ early fluorescence can be precluded because this will make the intensity of the initial $(dA)_{20}$ spectrum decrease by ~80% in comparison to the Ado counterpart as a result of the small fraction of the unstacked adenine units (~20%) in the $(dA)_{20}$ oligomer. The observed ~15% decrease in the fluorescence intensity of $(dA)_{20}$ can be readily associated with the hypochromism suffered by $(dA)_{20}$ relative to Ado. This general similarity exhibited by the initial Ado and $(dA)_{20}$ fluorescence spectra is compelling evidence for an excitation of localized nature for the $(dA)_{20}$ Franck−Condon (FC) state; i.e., the 267 nm excitation of $(dA)_{20}$ produces an excited state initially localized on a single adenine constituent.

The resemblance in the Ado and $(dA)_{20}$ initial KTRF spectra also helps to rule out any significant contributions from excitation of any probable adenine stacked complexes associated with the microscopic heterogeneity of the $(dA)_{20}$ oligomer. This is based on the consideration that, relative to the spectra from the base monomer, the stacked complexes generally display deeply red-shifted fluorescence excitation and fluorescence emission spectra.[26,39] For example, the excitation/emission λ_{max} of certain stacked complexes of an adenine polymer were found to be at 320 nm/420 nm in poly (A) in comparison to the corresponding ~260 nm/310 nm in Ado.[26] If the stacked complex(es) were involved to any substantial extent, a significantly weakened and strongly red-shifted initial fluorescence profile would be expected which is not observed in our KTRF results.

For the two red-shifted and longer-lived $(dA)_{20}$ fluorescence components, the explicit absence of their counterparts in the Ado spectra indicates that they are from excited states (denoted as E_1 and E_2 state, respectively, for the ~4.3 ps and ~182 ps components) formed due to the interbase stacking interaction. We note that the E_1 (Figure 3e) and E_2 (Figure 3f/g) fluorescence

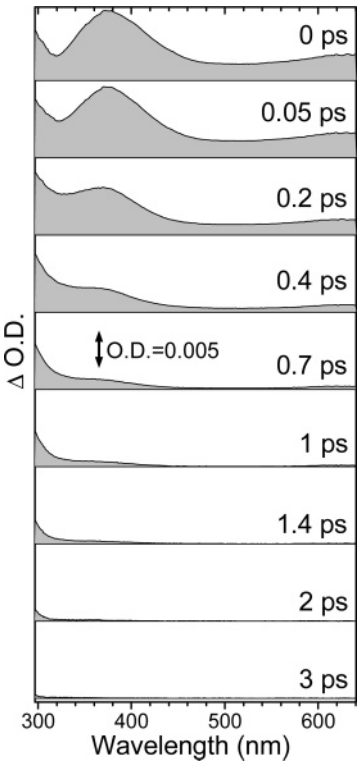

Figure 5. Temporal evolution of transient absorption spectra obtained for Ado with 267 nm excitation in an aqueous solution.

observed here are quite similar in spectral profiles to the two fluorescence components reported by Plessow and co-workers for a photoexcited adenine 15-mer using a wavelength- and time-resolved streak camera technique.[15] However, due to the relatively low time resolution (about 40 ps) and their limited spectral detection window, the strong ultrafast UV region fluorescence component revealed clearly by our KTRF experiment were not observed in their measurements. It is important to note that, according to the local excitation nature revealed for the initially excited $(dA)_{20}$, the E_1 and E_2 states should be produced with the excited adenine constituent as a precursor. This strongly favors their identities as the "excimer" (spanning two adjacent bases) or "excimer-like" (involving more than two bases) states[13,15,20] rather than the excited states of statically stacked complexes.[19,26,39] However, due to the weakness of the E_1 and E_2 fluorescence in comparison to the strong initial fluorescence, it is difficult to exclude unambiguously the possibility that either one or both the two fluorescing components may stem from direct excitation of very low concentrations of certain statically stacked complex(es). To exclude this possibility as well as to explore whether there are additional "dark" excited states included in the excited-state relaxation pathway, we present below our broadband TA results for Ado and $(dA)_{20}$.

C. Femtosecond Broadband Transient Absorption (TA) Spectroscopy. Representative TA spectra recorded at typical time delays are displayed in Figures 5 and 6, respectively, for Ado and $(dA)_{20}$. Consistent with the KTRF spectra of Ado and $(dA)_{20}$, the TA spectra of Ado and $(dA)_{20}$ are essentially identical to one another at very early times (around 0 ps). The initial Ado TA spectrum decays rapidly within several picoseconds but the corresponding $(dA)_{20}$ spectrum evolves into an alternative profile with its peak position shifted more to the blue. This

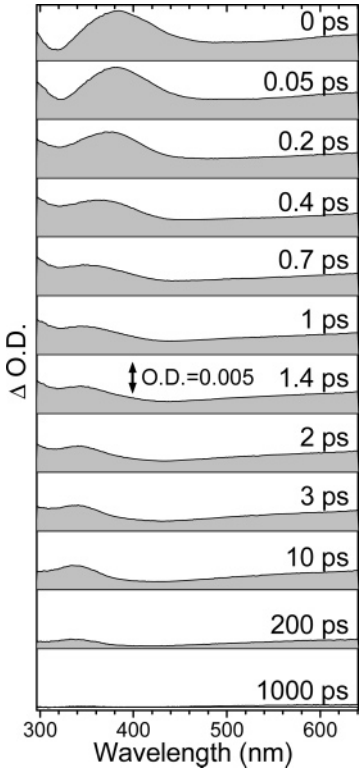

Figure 6. Temporal evolution of transient absorption spectra obtained for $(dA)_{20}$ with 267 nm excitation in an aqueous solution.

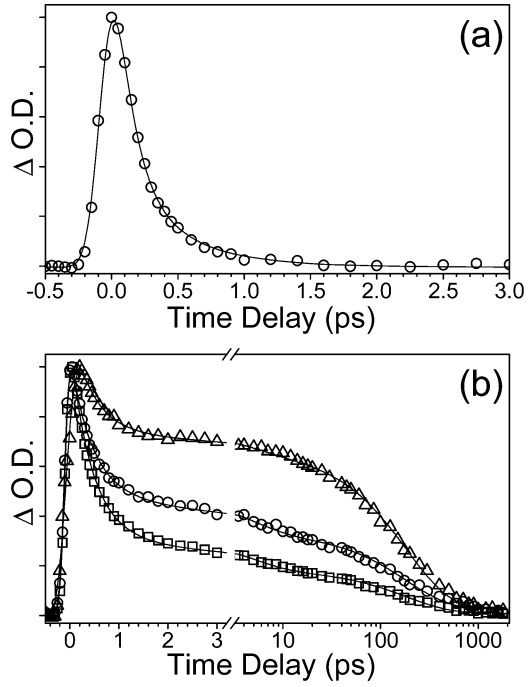

Figure 7. Time-dependence of the excited-state absorption decay for Ado (a) at 440 nm and $(dA)_{20}$ (b) at 340 nm (△), 400 nm (□), and 440 nm (○) obtained from the TA spectra in Figures 5 and 6, respectively. Solid lines are from the IRF convoluted two (for Ado) and three (for $(dA)_{20}$) exponential function fittings of the corresponding experimental data (see the text for details). The $(dA)_{20}$ data with time delays before and after 3 ps are displayed, respectively, on a linear and logarithmic time axis.

spectrum then decays with a time scale matching the longest excited-state decay dynamics observed in the $(dA)_{20}$ KTRF spectra (see Figure 3). Global dynamics analysis indicates that the temporal decays of the visible region (400−650 nm) Ado spectrum and the overall spectral region of the $(dA)_{20}$ spectrum can be described, respectively, by the same two (with 0.13 and 0.45 ps time constants)[47] and three (with 0.39, 4.3, and 182 ps time constants) exponentials revealed by the KTRF dynamics fittings. Representative decay dynamics of the TA spectra at various wavelengths are displayed in Figure 7a and b for Ado and $(dA)_{20}$, respectively. The general agreement in the spectral evolution dynamics displayed by the TA spectra and their corresponding KTRF spectra indicates that both of these measurements are probing the same excited-state processes for the two compounds. Thus, the TA spectra and related KTRF spectra can be attributed to the same pertinent excited-state species.

One may note that temporal evolution of the Ado TA spectrum reveals a gradually slower decay as the wavelength changes from 400 to 310 nm. This wavelength dependent dynamics in the blue region in conjunction with the more rapid decay dynamics in the visible region corroborates and substantiates the ultrafast deactivation mechanism proposed previously for photoexcited nucleobases, -sides, and -tides.[4,5−12,31−34] The blue region spectral evolution is due to the combined contributions of the excited-state deactivation and population relaxation of the vibrationally hot S_0 ground state (signified mostly by the spectra with time delays after 0.4 ps). The rapid deactivation IC process dumps most of the absorbed photoenergy into the recovering ground-state molecules making them vibrationally highly excited, and this induces extensive broadening of the S_0 absorption spectral profile toward the lower energy region.[4−6] Therefore, compared to the normal S_0 absorption that ends at ∼290 nm (see Figure 1), the hot S_0 TA spectra extend further down to ∼400 nm. From our TA spectra, the wavelength-dependent cooling time can be estimated to be roughly ∼0.41, ∼0.55, and 0.82 ps, respectively, at the 340, 320, and 300 nm wavelengths. The time constant obtained at 340 nm coincides with the cooling time constant of 0.4 ps at the same wavelength reported in an earlier TA study by Kohler and co-workers.[5b] According to the ground-state recovery dynamics monitored at the UV wavelengths of 250 and 270 nm (beyond our fs-TA detection window), an overall time constant of ∼2 ps has been determined for cooling of the vibrationally hot ground state by energy transfer to the surrounding solvent.[5b,13a]

Temporal evolution of the $(dA)_{20}$ TA spectrum (see Figure 6) is also characterized by obvious changes in the spectral profile in the 310−400 nm region. However, this spectral transformation is associated mostly with the excited-state dynamics rather than the ground-state cooling seen in Ado. This is indicated unequivocally by the good correlation of the spectral decay dynamics with the corresponding KTRF dynamics as well as the remarkably slow spectral decay and the absence of the characteristic cooling associated changes in the spectral profile for the spectra at later times. From comparison of the corre-

(47) The Ado TA deactivation decay in the visible region can also be fit roughly by a one-exponential function, and the 0.23 ± 0.02 ps time constant determined for the 570 nm wavelength is close to the 0.29 ± 0.04 ps value reported at this wavelength in ref 5b. We found however that the time constant obtained from the single-exponential fitting is close to the average time constant (∼0.20 ps at 570 nm) obtained from the two-exponential fitting. From this and the very similar excited-state dynamics displayed by the corresponding TA and KTRF spectra, we consider the single-exponential TA time constant being the weighted mean of the two exponential time constants determined from the KTRF dynamics (Figure 2b). We therefore think it is unlikely that one alternative excited state is responsible for the observed TA spectra, though, in some other cases, the TA and KTRF measurements may detect electronic transitions of different excited states.

sponding TA and KTRF spectra, it is clear that the very early TA spectra (at 0 and 0.05 ps) are from the local excited state of the adenine constituent and that the later time spectra are due to the E_1 (spectra at early picosecond time delays) and E_2 (spectra at 10 ps and after time delays) excited states. Our results are consistent with and correlate well with the previous fs-ESA study by Kohler and co-workers[13a] that shows a high yield of the long-lived excited state after 266 nm excitation of an adenine 18-mer with only a small fraction of the excited-state population channelling into the S_0 state by the ultrafast IC deactivation pathway. As a result of the small population, the hot adenine S_0 state may contribute only a small fraction to the blue region $(dA)_{20}$ TA spectra and thus introduce only a very small perturbation to the subpicosecond dynamics. Thus, the overall TA spectral evolution in this spectral region can still be well described by the excited-state dynamics. The ~182 ps lifetime estimated here for the E_2 state is comparable to the ~126 ps/~154 ps lifetime reported by Kohler and co-workers for the long-lived excited state of adenine 18-mer/polymers[13] indicating we are monitoring the same excited state. From the temperature-dependent efficiency, Kohler and co-workers have associated this state with the "excimer" state with excitation delocalized over two or more adenine components.[13(b)] However, due to the lack of wavelength-resolution in most of previous relevant time-resolved studies,[13,14] the ~4.3 ps E_1 state that is time-resolved and spectrally resolved in our KTRF and TA spectra has not been identified and reported in the literature to the best of our knowledge.

The close similarity in the initial TA spectra of Ado and $(dA)_{20}$ coincides with the corresponding KTRF comparison and strengthens the local excitation description ascribed above to the initial state of photoexcited $(dA)_{20}$. We note there is sizable intensity in the E_1 and E_2 states of the TA spectra (spectra at 2 and 10 ps, respectively in Figure 6) relative to the initial TA spectrum (spectrum at 0 ps in Figure 6). In addition, the TA spectral profiles exhibited by the two excited states (E_1 and E_2) are different from that of the initial Ado spectrum (spectrum at 0 ps in Figure 5). These preceding two observations and the close resemblance of the early Ado and $(dA)_{20}$ TA spectra also represent convincing evidence to indicate the dynamical origin of the E_1 and E_2 states. The time zero TA spectra of the E_1 and E_2 state deduced by extrapolating the corresponding TA spectra back to a zero time delay have more than half the intensity of the early $(dA)_{20}$ spectrum (at 0 ps time delay) in the 310−400 nm spectral region. In case either or both of these states were populated directly by the photoexcitation, one would expect the initial $(dA)_{20}$ TA spectrum to have a profile substantially different from the early Ado TA spectrum. This is obviously not observed in the experimental data and clearly indicates that the E_1 and E_2 states are not initially photoexcited but are formed subsequently from the initially populated local "A-like" state. In addition, the absence of a ground-state recovery component with a time constant correlating to the E_1 lifetime[13a] may suggest that evolution into the E_2 state could be the major deactivation channel of the E_1 state.

Based on our steady-state and time-resolved results for $(dA)_{20}$ and its comparison with Ado as well as correlation of the ground-state recovery and excited-state decay dynamics reported by others previously for the relevant adenine oligo- and polynucleotides,[13] we suggest the following consecutive deactivation scheme for the 267 nm excited $(dA)_{20}$: the photoabsorption leads to formation of the A-like state with excitation localized on one adenine constituent; except for a small fraction that decays to the S_0 state by ultrafast IC, most of the "A-like"-state population transforms into the E_1 state through interaction with neighboring base(s) with a time constant close to ~0.34 ps; the E_1 state is then further stabilized and evolves into the E_2 state with a ~4.3 ps time constant; accompanied by emitting the ~390 nm (λ_{max}) weak and red-shifted fluorescence, nonradiative deactivation of the E_2 state finally brings the excited-state population back to the S_0 state with a lifetime of ~182 ps. A scheme consistent with such a relaxation pathway is shown in Figure 8b. We note that previous time-dependent studies on adenine oligo- and polynucleotides have reported a long nanosecond decay component.[4,15,24,39a] Besides the subpicosecond and picosecond components, our KTRF and TA experiments also found a very weak and offsetlike signal persisting at longer time scales, which cannot be well characterized in our present measurements. Considering the general consistence between the steady-state and time-resolved fluorescence results as well as the reported almost total recovery of the ground-state bleach accompanied by a decay of the "excimer-like" state,[13a] it is reasonable to suggest that any longer component, if it does exist, would not contribute significantly to the excited-state relaxation process.

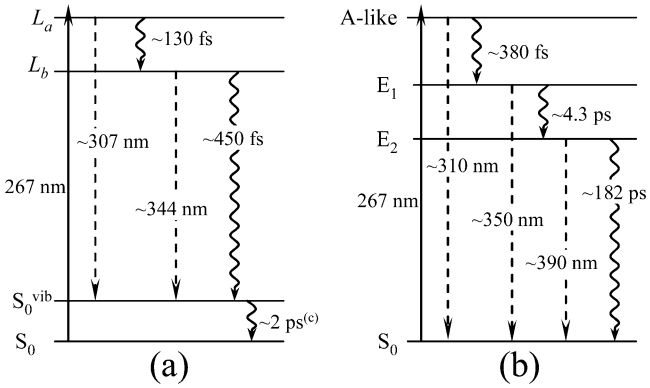

Figure 8. Schematic energy diagrams showing the proposed major population relaxation pathways for the 267 nm photoexcited Ado (a) and $(dA)_{20}$ (b) in an aqueous solution. [(c)]From refs 5b and 13a. The dashed arrow lines with the wavelength values indicate the fluorescence deactivation of the corresponding states; the curved lines indicate the nonradiative deactivation pathways with the corresponding decay times of the relevant excited states.

Discussion

A. Assignment and Deactivation Mechanism of Photoexcited Adenosine. To better understand the remarkably different excited-state dynamics displayed by Ado and $(dA)_{20}$, it is necessary to gain further insight into the nature of the emitting states. We discuss first the excited state(s) of the Ado monomer. The 267 nm excitation of Ado reaches the lowest close-lying L_a and L_b $\pi\pi^*$ excited states of the adenine moiety.[9,10,12,28d,31−35] The upper L_a transition is strongly allowed and carries most of oscillator strength, and the lower L_b state is relatively weakly allowed and may vibronically mix with the L_a state. It is straightforward to consider that the observed biexponential fluorescence decay may indicate involvement of both the L_a and L_b states to jointly account for the observed fluorescence spectra (see Figure 2). In this context, we have decomposed

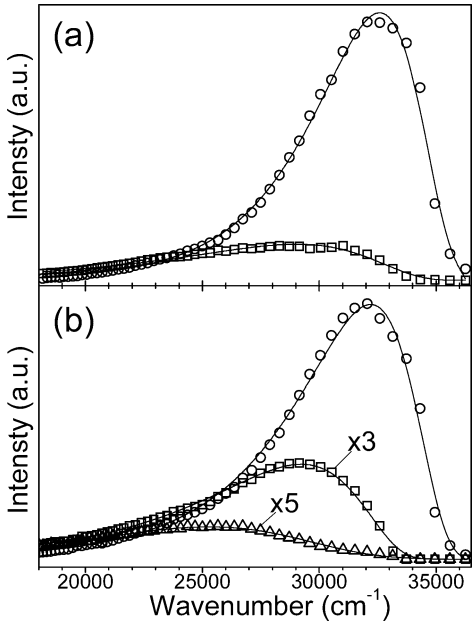

Figure 9. Fluorescence spectra acquired from KTRF decay analysis for the L_a (○) and L_b (□) state of Ado (a) and the A-like (○), E_1 (□), and E_2 (△) states of $(dA)_{20}$ (b) in an aqueous solution. Solid lines are from the log-normal simulation of the corresponding spectra (for details see the text). To display the spectra clearly, the intensity of the E_1 and E_2 spectra have been enlarged by 3 and 5 times, respectively.

the Ado absorption spectrum (Figure 1) by a log-normal function into two components corresponding to the L_a and L_b transitions (see Figure 4S in the Supporting Information) with their corresponding transition energies and oscillation strengths referring to the published experimental values.[35] We have also obtained the L_a and L_b intrinsic fluorescence spectra from the fitting coefficients determined by a fluorescence decay analysis at various wavelengths (see Supporting Information for details). These spectra are displayed in Figure 9a. The much higher L_a than L_b fluorescence intensity reflects the much stronger oscillator strength of the former than latter transition, and this agrees with their assignments to the L_a and L_b states, respectively. Employing this assignment, an overall fluorescence quantum yield of 0.56×10^{-4} can be estimated based on the integration area of the fluorescence spectra, the measured fluorescence lifetimes, and the intrinsic L_a radiative rate constant derived according to the Strickler−Berg correlation[48] between the decomposed L_a absorption and fluorescence spectrum (for details see the Supporting Information). The relevant data are compiled in Table 1. Clearly, the estimated quantum yield is very close to the reported experimental value of 0.6×10^{-4}. This good agreement justifies the above analysis and confirms the significance of the two $\pi\pi^*$ states to account for the observed Ado two-exponential fluorescence decay dynamics. Considering that the transition dipoles related to the L_a and L_b emissions are oriented in different directions,[12,31−34,35,] this may also explain the substantially lower value of the early time fluorescence anisotropy observed in the adenine nucleoside.[9] We note that, based on the steady-state UV absorption and Strickler−Berg analysis, Kohler and co-workers also proposed the importance of the two lowest $\pi\pi^*$ states to account for the emission of purine nucleosides.[49] Our results here represent the first excited-state analysis based on the directly observed transient fluorescence spectrum.

From our combined TA and KTRF results, a deactivation mechanism including only the L_a and L_b $\pi\pi^*$ states can be constructed for the ultrafast irradiative relaxation of photoexcited Ado in an aqueous solution. The possible involvement of additional excited state(s), such as the "dark" $n\pi^*$ and/or $\pi\sigma^*$ state(s), within the deactivation pathway can be excluded by the above fluorescence analysis and the observation that the hot ground-state absorption appears on the same time scale as the decay of the excited-state absorption and fluorescence. The correlation between the ground-state and excited-state dynamics and the lack of a photochemical reaction also help to rule out the probable source of intermolecular reactions (such as proton or hydrogen exchange between the excited adenine chromophore and surrounding solvent molecules[4]) to the observed excited-state dynamics. Our proposed Ado deactivation description is as follows (see Figure 8a): after excitation into the L_a state, ultrafast water solvation (that occurs on the ∼50 fs time scale)[50] and vibrational relaxation[5,51−53] (processes being too fast to be resolved by our experiment) bring the molecule to the L_a minimum; the L_a-state molecule then evolves by internal conversion to the L_b minimum with a ∼0.13 ps time constant, and this is followed by decay of the L_b state directly into the S_0 state creating a vibrationally hot S_0 state cooled by energy transfer to the solvent environment.[5] This mechanism is supported by recent theoretical studies[12,32−34] showing there is a strong coupling between the L_a and L_b states and the existence of a virtually barrierless depopulation channel for the L_b potential surface to convert into the ground-state surface through a conical intersection. These calculations also indicate there is an essential out-of-plane conformational change of the adenine aromatic ring to access the conical intersection so as to deactivate the excited state.[12,32,33] It is interesting to mention that the fairly large Stokes shift (∼6000 cm^{-1}) displayed by the fluorescence/absorption (see Figures 1 and 2) spectra may reflect not only the large extent of solvent stabilization due to the increased excited-state dipole moment but also significant structural changes in the excited states compared to the ground state.[4,12,21−34,36]

The deactivation mechanism proposed here is noticeably different from the corresponding gas-phase mechanism. Many recent studies have presented convincing evidence for the involvement of the lowest $n\pi^*$ state in the gas-phase deactivation pathway and emphasized the importance of this state as being responsible for the excitation wavelength dependence of the gas-phase deactivation dynamics for adenine and relative derivatives.[10,12,32−34] Various previous studies indicate consistently that the adenine $n\pi^*$ state is buried under the strong ∼260 nm absorption with an energy close to the L_a and L_b states.[4,10,12,32−34,35] The energy gap and relative order of the $n\pi^*$ vs the $\pi\pi^*$ states can be sensitively controlled by the environmental medium.[30a,35,36] The discrepancy between the gas phase and solution phase mechanism can be understood in terms of a well-known solvent effect:[4,30a,36,54−58] the $n\pi^*$ state is stabilized less effectively by an increasing solvent polarity and H-bonding in comparison to

(48) Strickler S. J.; Berg, R. A. *J. Chem. Phys.* **1962**, *37*, 814−822
(49) Cohen, B.; Crespo-Hernández, C. E.; Kohler, B. *Faraday Discuss.* **2004**, *127*, 137−147.
(50) Jimenez, R.; Fleming, G. R.; Kumar, P. V.; Maroncelli, M. *Nature* **1994**, *369*, 471−473.
(51) Laubereau, A.; Kaiser, W. *Rev. Mod. Phys.* **1978**, *50*, 607−665.
(52) Elsaesser, T.; Kaiser, W. *Annu. Rev. Phys. Chem.* **1991**, *42*, 83−107.
(53) Stratt, R. M.; Maroncelli, M. *J. Phys. Chem.* **1996**, *100*, 12981−12996.

the $\pi\pi^*$ states and the ground state. This leads to an energy increase of the $n\pi^*$ state relative to the $\pi\pi^*$ states in the solution phase, and this can make it energetically inaccessible for the relaxation process.[32,33] Since water is a solvent with an extraordinarily high polarity and a strong H-bonding capacity,[57] this effect is expected to work most notably in an aqueous solution. The lack of the $n\pi^*$ state in the aqueous solution deactivation pathway is also consistent with a very recent fs up-conversion TRF study by Pancur and co-workers.[9] This study found that, in contrast to the gas-phase excitation wavelength-dependent deactivation dynamics, the aqueous solution Ado deactivation is almost independent of the excitation wavelength.[9] This difference in the solution vs gas-phase deactivation pathways reflects the sensitivity of the deactivation channel and dynamics to the local environment of the molecule.

We note that recent theoretical studies by Sobolewski and co-workers propose that a $\pi\sigma^*$ state plays a crucial role in the ultrafast IC deactivation of the electronically excited adenine and other heterocyclic aromatic molecules in the gas phase as well as in the solution phase.[59] According to this model, deactivation through a predissociation of the optically excited $\pi\pi^*$ state and a conical intersection with the ground state occurs where the $\pi\sigma^*$ state mediates the rapid IC deactivation and thus accounts for the photostability of the biomolecules. In 9-H adenine, the lowest $\pi\sigma^*$ state was identified to be dissociated along a stretching coordinate of the N9−H bond.[59] Such a $\pi\sigma^*$ mechanism has been invoked to interpret the detection of H-atom loss in UV-light excited adenine in recent gas-phase measurements.[60] However, based on the results of a similar excited-state lifetime observed for low UV-excited adenine and its various deuterated and methyl-substituted derivatives in the gas phase, Kim and co-workers ruled out the possibility of IC via the $\pi\sigma^*$ state potential surface along the N9−H bond and argued against the special role of the $\pi\sigma^*$ state.[61] The subpicosecond IC dynamics determined here and by others[5b,8] for Ado in aqueous solution and the similarly rapid deactivation dynamics reported for 9-H adenine and 9-methyladenine (9MA) in water[5c] indicate also that the ultrafast IC relaxation occurs irrespective of the presence of the N9−H coordinate. This combined with our proceeding Ado fluorescence yield and dynamics analysis appears to imply only a minor importance of the $\pi\sigma^*$ state in the 267 nm excited Ado IC relaxation processes.

B. Deactivation Pathway of Photoexcited $(dA)_{20}$. For $(dA)_{20}$, a preliminary analysis based on the corresponding KTRF spectra and the proposed cascade population relaxation mechanism (Figure 8b) have been done to deduce the intrinsic fluorescence spectra for the three fluorescence components. The spectra obtained from the fitting coefficients determined by the three exponential simulation of the fluorescence decay at each wavelength (see the Supporting Information for details) are displayed in Figure 9b. From the ratio of the spectral area and assuming a 70% conversion efficiency[13a] from the "A-like" to the E_1 and E_2 states, one can estimate roughly that the intrinsic radiative rates of the E_1 and E_2 states are ∼5 times and ∼20 times, respectively, weaker than that of the "A-like" fluorescence. These results combined with the measured lifetimes can then be used to infer that ∼9% and ∼87% of the $(dA)_{20}$ fluorescence quantum yield are contributed by the E_1 and E_2 fluorescence, respectively, and the remaining ∼4% is due to the "A-like" fluorescence. Considering the "bright" nature of the "A-like" fluorescence, the much weaker fluorescence cross-sections for the E_1 and E_2 states are in agreement with the generally suggested charge transfer and charge resonance character of aromatic excimers[4,13a,25,26] and is consistent with the assignments of the E_1 and E_2 states to "excimer" and "excimer-like" states. From the very close similarity between the Ado and $(dA)_{20}$ initial spectra (both the KTRF and TA spectra), it is reasonably certain that 267 nm excitation of $(dA)_{20}$ is, like the Ado case, due to the highly allowed L_a transition of the adenine constituent. However, our present data do not allow further unambiguous correlation of this fluorescence to any specific electronic transition(s). To avoid an arbitrary assignment and bearing in mind many of the relevant complexities to the "A-like" fluorescence (such as spectral inhomogeneities due to the involvement of both the stacked and unstacked adenine and probable differences in the local environment), we only note here that the associated electronic transition(s) should have a similar intrinsic electronic configuration(s) as that of the Ado $\pi\pi^*$ excited states (the L_a and/or mixed with L_b character). We therefore tentatively regard the "A-like" fluorescence of $(dA)_{20}$ as being from a single "A-like" excited state of the adenine constituent, whose further deactivation channel and dynamics depends highly on the details of the local stacking conformation. Based on this and the respective lifetime and corresponding fluorescence quantum yield, one can estimate the intrinsic radiative rate for the "A-like", E_1 and E_2 states and these results are listed in Table 1.

Compared to Ado in aqueous solution, the stacked adenine $(dA)_{20}$ in aqueous solution senses not only the solvation due to the surrounding water molecules but also an extra stacking interaction induced by the neighboring base(s). The local excitation character identified here for the initially excited $(dA)_{20}$ implies that the additional interbase interaction is rather weak in the ground state (manifesting itself mainly as Columbic interactions)[20,37,44−45] so that it has little influence on the intrinsic character of the related electronic transition. We note that the local excitation description was hypothesized in some early studies of DNA photophysics[1,4,20] to explain the general observation that the absorption spectrum of any given base multimer closely resembled the overlap of the constituent base spectra. However, by showing that the absorption spectral correlation is not inconsistent with the FC excited states with an excitation delocalized over several bases, this description has been challenged recently by several theoretical studies.[35] In this context, the results here provide the first definitive

(54) Scaiano, J. C. *J. Am. Chem. Soc.* **1980**, *102*, 7747−7753.
(55) Dalton, J. C.; Montgomery, F. C. *J. Am. Chem. Soc.* **1974**, *96*, 6230−6232.
(56) Rusakowicz, R.; Byers, G. W.; Leermakers, P. A. *J. Am. Chem. Soc.* **1971**, *93*, 3263−3266
(57) Reichardt, C. *Solvent and Solvent Effect in Organic Chemsitry*; VCH: Verlagsgesellschaft mbH, D-6940, Weinheim, 1988.
(58) (a) Kim, N. J.; Kang, H.; Jeong, G.; Kim, Y. S.; Lee, K. T.; Kim, S. K. *J. Phys. Chem.* **2000**, *104*, 6552−6557. (b) Kim, N. J.; Jeong, G.; Kim, Y. S.; Sung, J.; Kim, S. K.; Park, Y. D. *J. Chem. Phys.* **2000**, *113*, 10051−10055. (c) Kang, H.; Lee, K. T.; Kim, S. K. *Chem. Phys. Lett.* **2002**, *395*, 213−219.
(59) (a) Sobolewski, A. L.; Domcke, W. *Eur. Phys. J. D* **2002**, *20*, 369−374. (b) Sobolewski, A. L.; Domcke, W.; Dedonder-Lardeux, C.; Jouvet, C. *Phys. Chem. Chem. Phys.* **2002**, *4*, 1093−1100.
(60) (a) Zierhut, M.; Roth, W.; Fischer, I. *Phys. Chem. Chem. Phys.* **2004**, *6*, 5178−5183. (b) Hünig, I.; Plützer, C.; Seefeld, K. A.; Löwenich, D.; Nispel, M.; Kleinermanns, K. *ChemPhysChem* **2004**, *5*, 1427−1431.
(61) Kang, H.; Jung, B.; Kim, S. K. *J. Chem. Phys.* **2003**, *118*, 6717−6719.

experimental evidence to justify a localized excitation feature for photoexcited base multimers.

The quick and predominant conversion of the local "A-like" state into the E_1 "excimer" state observed here implies that the interbase electronic coupling of the excited base component with neighboring base(s) enables the intermolecular process of the "excimer" formation to compete effectively with the intramolecular irradiative IC process available to a single base unit. The much stronger interbase coupling in the excited state than in the ground state may come from not only the increased dipole−dipole interaction (as expected by the increased dipole moment of the excited state(s) relative to the ground state[12,32−34,36]) but also and more importantly from the orbital overlap and probably covalent bonding between the interacting bases.[4,20] The base stacking conformation is crucial in this regard: on one hand, by keeping the adjacent bases in close contact (about ∼3.4 Å apart) and parallel to one another,[4,37−39] the base stacking may facilitate the π electron overlap and assist covalent bond formation; on the other hand, by exerting a conformation constraint and especially restraining the kind of out-of-plane structural change required for accessing the conical intersection region,[12,32−33] the base stacking may help to prevent and block the intramolecular irradiative channel. Since the subpicosecond conversion time (∼0.40 ps time constant) from the "A-like" to E_1 state is too short to allow any significant nuclear motion, it is reasonable to think that the creation of the E_1 "excimer" state occurs mostly by an electronic bonding process either based on the ground-state stacking conformation or mediated by only small changes in the conformation. Since the ground-state stacking construction may, in many cases, diverge, to a certain extent, from the idealized "sandwich" geometry required for producing a fully stabilized "excimer",[62] the rapid E_1 formation dynamics may have the following implications: (i) Charge transfer and charge resonance interaction may play an important role in driving and stabilizing the E_1 formation. (ii) The generation of the E_1 state represents only the first step of processes caused by the base stacking interaction. Subsequent stabilization or reaction of this state promoted by the relatively large-scale nuclear motion(s) permitted by the structural flexibility[63,64,65] of the stacking conformation may lead to a process occurring on a relatively slower time regime. (iii) The efficiency of the E_1 formation would be highly sensitive and controlled by the ground-state base stacking morphology. Implication (i) is based on the consideration that the steric requirement is not very strict for the charge transfer and the charge resonance interaction and that the preponderance of the charge-transfer interaction is expected to be high since electronic excitation lowers the ionization potential of the excited base relative to that of the ground-state base.[4,13,16,25] Indeed, the rapid stacking induced excited-state charge transfer to a neighboring base has been invoked as a mechanism for fluorescence quenching of oligomers containing 2AP.[16,66] The charge-transfer character was also invoked to explain the out-of-plane component observed in the emission polarization measurement for the adenine dimer and polymers.[25] For implication (ii), photoexcitation of $(dA)_{20}$ results in hardly any photoproduct, and we thus associate the ∼4.3 ps decay of the E_1 state with a structural reorganization process in terms of the conformational adaptation needed to achieve a favorable configuration for the creation of the fully stabilized and long-lived E_2 "excimer-like" state. Toward this end, the E_2 state may differ from the E_1 state by the degree of energy stabilization, which is responsible for the observed deeper fluorescence red-shift of the E_2 vs the E_1 state. The E_2 state may also differ from the E_1 state by the spatial extent of interbase coupling, i.e., the E_2 state may involve more than two base units.[4,13] Considering the fact that many oligo- and polynucleotides exhibiting the long-lived excimer state are actually photostable,[13a] it is interesting to propose that the photoreactivity and likelihood of photodamage of a certain base multimer (or DNA sequence) may not necessarily correlate with its ability to form the long-lived excited state but may instead be associated with the nature and reactivity of the E_1 type precursor as observed here for $(dA)_{20}$ which is highly sensitive to the peculiar electronic property and stacking conformation of the interacting base units. In this regard, the formation of some important photolesions such as the cyclobutyl pyrimidine dimer (CPD)[1−4,67] could probably occur rather quickly on the singlet manifold and on the picosecond time scale. In the case of implication (iii), the branching of the "A-like" excited state between conversion back to the ground state (for unstacked or inappropriately stacked base constituents) and into the longer-lived E_1 and then E_2 state (for appropriately stacked bases) would be governed by the oligomer stacking geometry. Due to the predominance of the E_1 and E_2 fluorescence to the overall fluorescence yield, this may imply a direct association of the stacking conformation to the fluorescence quantum yield. Combining implications (ii) and (iii) suggests that the fluorescence properties such as the yield and wavelength maximum may be taken as a probe for the oligomer stacking conformation and this may explain the significant influence of the secondary structure (controlled largely by the sugar−phosphate backbone conformation) on the fluorescence quantum yield and the fluorescence spectra of adenine dimer ApA and polymer poly(dA) and poly(A).[1,4,13(b)]

Conclusion

The advantages of femtosecond time resolution and a broad spectral and temporal probing window in our combined KTRF and TA experiments were employed to provide the first femtosecond real time comparative spectral characterization for the excited-state deactivation processes and relaxation dynamics of adenine monomer Ado and oligomer $(dA)_{20}$. Our results for Ado enable a distinct mechanism that includes the L_a and L_b $\pi\pi^*$ excited states to be proposed for Ado ultrafast irradiative deactivation in an aqueous solution. Comparison of the spectral evolution in the KTRF and TA spectra for Ado and $(dA)_{20}$ presents convincing evidence for the localized nature of the initial excitation of UV excited $(dA)_{20}$. The results also indicate

(62) Birks, J. B. *Organic Molecular Photophysics*; John Wiley & Sons, J. W. Arrowsmith Ltd.: Bristol, U.K., 1973; Vols. 1 and 2.
(63) (a) Gearheart, L. A.; Somoza, M. M.; Rivers, W. E.; Murphy, C. J.; Coleman, R. S.; Berg, M. A. *J. Am. Chem. Soc.* **2003**, *125*, 11812−11813. (b) Brauns, E. B.; Madaras, M. L.; Coleman, R. S.; Murphy, C. J.; Berg, M. A. *Phys. Rev. Lett.* **2002**, *88*, 158101-1-4. (c) Brauns, E. B.; Madaras, M. L.; Coleman, R. S.; Murphy, C. J.; Berg, M. A. *J. Am. Chem. Soc.* **1999**, *121*, 11644−11649.
(64) (a) Pal, S. K.; Zhao, L.; Xia, T.; Zewail, A. H. *Proc. Natl. Acad. Sci. U.S.A.* **2003**, *100*, 13746−13751. (b) Pal, S. K.; Zewail, A. H. *Chem. Rev.* **2004**, *104*, 2099−2123.
(65) Trifonov, A.; Raytchev, M.; Buchvarov, I.; Rist, N. M.; Barbaric, J.; Wagenknecht, H.-A.; Fiebig, T. J. *Phys. Chem. B* **2005**, *109*, 19490−19495.
(66) (a) Jean, J. M.; Hall, K. B. *Biochemistry* **2002**, *41*, 13152−13161. (b) Jean, J. M.; Hall, K. B. *Proc. Natl. Acad. Sci. U.S.A.* **2001**, *98*, 37−41.
(67) Marguet, S.; Markovitsi, D. *J. Am. Chem. Soc.* **2005**, *127*, 5780−5781.

the significance of base stacking for modifying the deactivation pathway and enabling the generation of the weakly emissive but longer-lived E_1 "excimer" and E_2 "excimer-like" states that involve two and likely more than two nearby bases, respectively. The ultrafast transformation of the localized excited state to the delocalized E_1 "excimer" state indicates that base stacking has the ability to mediate efficient excitation energy transfer through interbase electronic coupling. We think that the scenario of local excitation followed by rapid energy transfer to a neighboring base may operate generally in many other base multimer systems. In this context, the nature and reactivity of the consequently formed E_1 state could be crucial to determine whether the formation of "excimer" could act as a trap for the excitation energy or be a precursor to subsequent photochemical reactions leading eventually to base damage. Due to its photostability, the former is valid for $(dA)_{20}$ as manifested by evolution of the E_1 state into the further stabilized E_2 state that then eliminates the excitation energy by emitting the very weak and deeply red-shifted fluorescence. Since properties and reactivity of the E_1 type "excimer" state are expected to be highly sensitive to the electronic nature of the interacting bases and local environmental factors such as the stacking conformation, we plan to extend our combined KTRF and TA spectroscopic methods to study other base monomer and multimer systems in order to explore and possibly establish a dynamic link between the UV excitation and the photochemical and photophysical outcomes. In addition, we hope that the spectral and dynamics data presented here can help provide valuable experimental information for comparison purposes in order to aid the development of appropriate theoretical models to better describe the solution phase excited-state deactivation process of both the base monomer and multimer systems.

Acknowledgment. This research was done in the Ultrafast Laser Facility at the University of Hong Kong and supported by grants from the University of Hong Kong (Seed Funding Program for Basic Research 2006-07) to W.M.K. and the Research Grants Council of Hong Kong (HKU/7021/03P and HKU 1/01C) to D.L.P. and (HKU 7029/06P) W.M.K. W.M.K. thanks the University of Hong Kong for the award of a Research Assistant Professorship.

Supporting Information Available: Figure 1S illustrates the spectral subtraction procedure to acquire the transient absorption spectra for $(dA)_{20}$ and Ado with 267 nm excitation in an aqueous solution. Figure 2S displays the UV-melting profile obtained at 260 nm for single-stranded oligonucleotide $(dA)_{20}$ in an aqueous solution. Part A. Details of using a log-normal function to simulate the KTRF spectra for Ado and $(dA)_{20}$. Figure 3S displays a comparison of experimental and log-normal fitted typical transient KTRF spectra for Ado and $(dA)_{20}$. Table 1S lists the spectral parameters obtained from the log-normal simulation of the typical Ado and $(dA)_{20}$ KTRF transient fluorescence spectra. Part B. Fluorescence spectra determined for the Ado L_a and L_b states based on a dynamics analysis of the Ado KTRF spectra. Part C. Estimation of the overall fluorescence quantum yield for Ado based on the Strickler−Berg equation for the correlation of the steady-state UV absorption and measured KTRF spectra. Figure 4S displays an experimental and log-normal decomposed UV-absorption spectrum of Ado in an aqueous solution. Part D. Fluorescence spectra determined for the $(dA)_{20}$ "A-like", E_1 and E_2 states based on a dynamics analysis of the $(dA)_{20}$ KTRF spectra. This material is available free of charge via the Internet at http://pubs.acs.org.

JA0622002